Nayab Bushra, Timo Hartmann

Design optimization method for roof-integrated TSSCs

Design optimization method for roof-integrated TSSCs

Nayab Bushra [a,*], Timo Hartmann [a]

[a] Civil Systems Engineering, Technical University of Berlin, Gustav-Meyer-Allee 25, 13355 Berlin, Germany

Email addresses: nayabbushra@outlook.com (Nayab Bushra); timo.hartmann@tu-berlin.de (Timo Hartmann)

* Corresponding author: Email address: nayabbushra@outlook.com

Abstract

This paper proposes a two-step design optimization method for roof-integrated two-stage solar concentrators (TSSCs) as energy supply systems. The integration process of these systems with buildings is complex as several conflicting and multi-disciplinary concerns need to be addressed. Thus, the proposed approach is intended to be adaptable to informed decision-making processes in early design stages, and yet to be collaborative where several key stakeholders are involved. The method is an extension to our previously developed approach where the performance of roof-integrated TSSCs in several design scenarios is accessed along with multiple performance indicators by developing a parametric model and controlling a set of design inputs. In the current study, the proposed method is combined with a multi-objective design optimization method, aiming to optimize, building and TSSCs geometry. The method was validated in an illustrative case study of a single-family house (California) for a number of conflicting objectives e.g., maximization of direct normal solar irradiance (DNI) and annual average load match index (av.LMI), and minimization of covered roof area. The validation of the method shows a number of interesting results. The method enables the generation of performance-driven designs and searches for the most appropriate solutions, that can help to meaningfully support the decision-making process.

Keywords: two-stage solar concentrator; roof-integrated; parametric; multi-objective; design optimization; decision-making.

1 Introduction

The push for a less carbon-intensive built environment has led to several questions about how self-sufficient buildings should be designed. Sustainability-related issues can be addressed by working on building envelopes to maximize solar gains [1,2,3], and integrating advanced solar technologies [1,4,5,6,7]. In recent years, building-integrated photovoltaics (PVs) have gained significant interest in building energy research [2,3,8,9,10,11,12,13]. However, PVs are still behind the solar concentrators (using mirrors and a receiver to convert sunlight into usable energy) in many aspects. For instance, a PV requires two times more space than a concentrator to produce the same amount of energy (~ 550 kW), where space can be a critical factor, especially in urban areas [14]. Further, PV efficiency is very low (16–22%) [15] compared with concentrator efficiency (40%) [16]. Concentrators with high concentration ratios have high efficiency and energy yield and need a small-sized receiver [17,18,19,20,21]. Among several designs, two-stage solar concentrators (TSSCs) show 50% to 200% [18,19,20] more concentration ratio and require lesser (i.e., 77%) solar cells [21] compared with traditional concentrators. TSSCs are prominent for high energy yield, efficient power delivery, and deployment modularity [22,23,24]. In TSSCs, light is reflected from a primary mirror to a secondary mirror, which is focused on the receiver [22]. Despite growing interest in building-integrated concentrators [25], there exists less research [24,26,27,28,29,30,31,32,33] on integrating TSSCs with buildings. Further, the integration of TSSCs with buildings reflects a complex decision-making process, involving stakeholders from different domains e.g., building architects, civil engineers, and energy specialists having multiple and conflicting objectives e.g., energy demand vs. energy yield vs. energy cost [2,34]. To address this, design optimization can help to find trade-offs and support the quick decision-making process. This facilitates the setup of design parameters (decision variables) and fitness functions (design objectives) for generating, evaluating, and optimizing multiple designs. Design optimization can be achieved by applying optimal combinations of different design strategies and ranking design options according to a set of objectives [35]. Nevertheless, design optimization for building integrated TSSCs requires optimization at the building level and system design level.

On the design level, TSSCs have several limitations e.g., complex architecture, the requirement of efficient trackers, poor performance in case of misaligned mirrors, and the requirement of high-

manufacturing skills [22]. Some studies [26,27,29] optimized TSSCs for minimum size and cost and maximum yield by considering decision variables e.g., the number of modules and arrangements, and receiver properties. However, there is still more research needed to include several other decision variables in the optimization process that include but are not limited to geometric concentration ratio [24], mirrors' size [31,33], the distance between mirrors [24,33], or the mirrors' shape [30,36] to generate optimal TSSC solutions. Additionally, the research on optimization of building-integrated TSSCs is scant [26,27,29]. Unlike PVs, TSSCs have the leverage of design flexibility (e.g., by varying mirror shapes, system dimensions, etc.) since the technology is still far from maturity [22]. Because concentrators only work under direct normal irradiance (DNI) unlike PVs. Thus, successful integration of TSSCs with buildings requires exploration of building surfaces that receive most of DNI, to ensure optimal performance of these systems. However, in existing research [26,27,29], building-integrated TSSCs are optimized as stand-alone designs before installation on buildings and are limited to existing buildings. Thus, building-related parameters are ignored for optimization of TSSCs while buildings control a significant proportion of incoming sunlight [2,3,8,9,10,11,12,13]. Hence, optimization of building surfaces, especially roofs that are more optimal locations in urban areas, is still missing for maximization of DNI, before installation of TSSCs.

This research envisions that design optimization of both; TSSCs and building can enable informed decision making, by generating several solutions and evaluating across different objectives. In this sense, the building roof can be optimized to maximize DNI, and TSSC geometry can be optimized for optimal performance. One possibility is to develop parametric models by mimicking design parameters [37] and applying multi-objective optimization [26,38,39] where *genetic algorithm* (GA) based methods are widely adopted in the buildings and energy research [26,39]. In the current research, there exist several parametric models combined with multi-objective optimization to maximize solar gains on building envelopes, ultimately energy yield [2,3,8,9,10,11,12,13]. To the authors' best knowledge, no study proposed any model to maximize DNI by applying parametric modeling and multi-objective optimization approaches. Existing models [2,3,8,9,10,11,12,13] enabled building design optimization, by mimicking building-related decision variables e.g., roof design and slope, or orientation. However, these models are limited to integrating PVs with buildings. Further,

these models are limited to using fixed, and commercially available PVs, and do not include PV-related decision variables.

To the authors' best knowledge, there exists no parametric modeling approach combined with multi-objective optimization for building-integrated TSSs considering building- and TSSCs-related decision variables, thus a collaborative design optimization of both is still missing. This motivates to development of an integrated design optimization approach in subsequent steps: optimization of roof design for maximizing DNI followed by optimization of TSSC design for improved performance. To begin to address this knowledge gap, this paper introduces a two-step design optimization method that allows for automatically integrating TSSCs with building roofs. The proposed method is based on our previously developed performance assessment method [40] of roof-integrated TSSCs, where several design alternatives were developed by applying a parametric modeling approach. Previously [40], we accessed the performance of roof-integrated TSSCs by manipulation of the building- and TSSCs-related design parameters i.e., roof shape, roof slope, building orientation, TSSC type, geometric ratio, and separation distance between mirrors. However, we did not optimize these designs through optimization algorithm(s), and manually filtered designs according to performance criteria. The method presented in this study enables a two-step optimization: (1) optimizing the roof design to maximize DNI (single-objective), and (2) optimizing TSSC configuration for two performance objectives (multi-objective): maximize energy reflected by annual average load match index (av.LMI) [41,42] and minimize covered roof area by TSSC modules. The proposed method applies NSGA-II (GA algorithm) due to its wide applications in the design optimization of buildings and energy systems [43,44,45,46]. In the proposed method, we consider decision variables that are related to both, building design (i.e., roof shape, slope, and orientation) and TSSC design (type, solar cell size, number of modules, geometric ratio, and separation distance between mirrors). Thus, our method helps us to find the best roof design achieving maximum DNI, and best TSSC designs that can be integrated well with buildings achieving maximum energy gain and requiring minimum installation space on the building's roof. The main hypothesis is that the performance of building-integrated TSSCs can be improved by applying parametric modeling and multi-objective optimization approaches to building scale, and TSSC scale

designs. The method presented in this research allows exploring trade-offs among performance objectives, enables performance-driven design, and serves to guide decision-makers.

The paper is structured as follows. Section 2 provides an overview of modeling and optimization considerations for installing TSSCs with buildings. We then describe the proposed method, highlighting the principal components of our approach in section 3. Section 4 represents the implementation of the proposed method in a case study. In section 5, we present our optimization results followed by the discussion and limitations of the proposed method in section 6. Finally, section 7 concludes the paper.

2 Background

Design problems related to building-integrated solar technologies are complex where conflicting goals are often required at the same time. This requires a holistic and integrated design approach where multiple teams can work together. Even in integrative and collaborative teamwork, finding a meeting point that allows the optimal solution for all necessities becomes challenging. Surely, suitable *multi-objective optimization* methods, aimed at tailored and reliable evaluations of the performance, are a possible answer where a range of solutions are sought that span the trade-off between each design objective [38,47]. In the field of building energy research, researchers usually define only two objectives, such as energy cost and CO2 emissions [43,48], energy use and cost [44], or energy use and daylight [35]. In a few cases, a few studies proposed three objectives such as [35], energy use, energy generation, and daylight [11], energy use, energy generation, and visual discomfort time [3], energy use, cost, and energy generation [2], or energy use, cost, and thermal comfort [10,49].

Nevertheless, a complex problem solving through multi-objective optimization usually covers two major aspects that includes: (1) optimization method, and (2) design optimization scope. Concerning the optimization method, evolutionary algorithms appear to resolve multi-objective optimization problems by mimicking the systems and techniques encountered in evolutionary biology [47]. In this context, concepts such as inheritance, mutation, natural selection, and crossover assist in the search for an optimal set of solutions to a given problem [47]. Several types of evolutionary algorithms have been identified in building energy research such as multi-objective genetic algorithm (MOGA) [50,51], micro-GA [26,27], fast non-dominated sorting genetic algorithm (NSGA-II) [43,44,45,46], multi-

objective evolutionary algorithms (MOE) [52], generalized pattern search optimization algorithms (GPSOA) [53], hybrid-GPSOA [54], and trust-region-reflective least-squares algorithms [55]. GAs are the population-based methods and have a good diffusion in the buildings and energy research community, producing a sub-optimal solution in a reasonable time where each individual of the population (decision variables) represents a solution for the target problem. The population of solutions evolves during several generations, where at each generation, all the individuals are evaluated by a fitness function that measures how good the solution represented by the individual is for the target problem [39]. Typically, the outcomes of multi-objective optimization are divided into feasible and Pareto solutions. Feasible solutions are found by the optimization algorithm in searching for optimal solutions, that satisfy all defined constraints. While a solution is Pareto optimal if there are no other feasible solutions that are better with respect to one objective without being worse with respect to at least one other objective [37]. In Pareto fronts, objectives can be mapped in single- or multi-dimensional representations, while the problems with more than three objectives are more challenging due to complexity of data to display [56]. The parallel coordinate plots are scalable alternative to plot optimization results. In general, number of generation and population size varies based on model complexity, where most studies reported generation size between 10 and 200, and population of 20 to 150 [10,11,35,44,45,48].

Regarding the design scope, during the multiple design stages of projects regarding the installation of solar technologies with buildings, several specialists need to interact concerning building and solar technology design to be integrated with building, to predict the overall performance across several disciplines. Typically, to achieve a sustainable building design, two main concerns are, how to design buildings to enhance solar energy yield [1,2,3], and how to design high-performing solar energy systems [6,7]. Although the optimization methods described above are undoubtfully promising, due to their inherent complexity, these methods are not commonly used in the design practice yet and currently are limited to a few academic research studies [35]. The complexity comes from the large number of multi-disciplinary interrelated parameters involved in optimizing building and system performance. Because of the high complexity in setting up a model for multi-objective optimization, there is a great demand for utilizing and integrating the advanced modeling and simulation

166 technologies, such as parametric models and optimization algorithms with energy simulations [35]. In
167 general, design optimization covers two aspects, choice of decision variables and selection of solar
168 technology. Typically, existing models take decision variables that are either related to building [1,2,3]
169 or energy systems [6,7]. However, there is a lack in considering the decision variables associated with
170 both, buildings, and solar technologies into a single framework. Moreover, in the process of integrating
171 solar technologies with building envelopes, one of the commonly developed approaches is the
172 parametric simulation method. This approach enables us to set design parameters within a proper
173 range and to see their effects on some objective functions, while other variables are constant [37].
174 Several studies proposed parametric models that were limited to optimization of building-integrated PV
175 systems [2,8,9,10,11,12,13]. Additionally, most of the fundamental work in this field is limited to
176 investigating the decision variables associated primarily with building geometries [2,8,9,10,11,12,13]
177 by manipulating roof forms, orientations, and roof slopes [2,3,57] aiming to increase the solar irradiance
178 and ultimately the energy yield from building-integrated solar energy systems. Regarding the
179 technology choice, PV systems are widely applied, however, there is little work towards practical
180 implementation of solar concentrators, in particular TSSCs, that are far better than PV in terms of their
181 performance.

182 In the current practice, for solar concentrators, design optimization is performed only for existing
183 buildings, not considering the optimization of building designs [26,27,45,46,53,55]. For instance,
184 studies aimed to optimize concentrator designs for maximizing energy yield or energy efficiency and,
185 minimizing the system cost, by investigating system-related design parameters such as mirrors'
186 diameter as well as operational parameters [45,53,58]. Considering other design approaches, TSSCs
187 have the advantage of higher yield by utilizing smaller-sized solar cells, over conventional single-stage
188 concentrators as highlighted in our previous study [40]. Despite their applications in buildings
189 [24,26,27,28,29,30,31,32,33], only a few studies reported design optimization models of TSSCs
190 integrated with buildings [26,27,29]. For example, Burhan et al. [26,27] optimized a TSSC design using
191 a micro-GA and aimed to find the optimum system configuration and dimension with zero failure time
192 and minimum cost. They [26] considered the module number and the initial storage as decision
193 variables. Later, they [27] incorporated other aspects e.g., solar cell (receiver) properties, and the

194 *optical parameters* and arrangement, and aimed to optimize the system size at minimum cost. Another
195 study [29] used a trust-region optimization algorithm to maximize electrical yield from a TSSC by
196 varying solar cell properties.

197 One of the major concerns in their successful implementation in the built environment is
198 optimizing TSSCs for several design-related and performance-related issues. Future cost-effective and
199 energy-efficient solutions can be developed by increasing energy yield and reducing the size of system
200 size [31,33] and solar cell receiver [21]. Further small or lesser modules can lead to reduction in energy
201 generation costs, especially in urban areas with significant space values [14]. Therefore, a significant
202 amount of effort is needed to design novel solutions by exploring several decision variables related to
203 design e.g., geometric concentration ratio [24], mirrors' size [31,33], the distance between mirrors
204 [24,33], or mirrors' shape [30,36]. However, an analysis of TSSCs for optimal performance by
205 considering all these parameters as decision variables is still missing in the current literature.

206 Considering building-integrated TSSCs, energy performance of TSSCs is not only influenced by
207 system design, but also building design achieving a certain DNI level. Therefore, the integration of
208 TSSCs with building also requires optimal building designs, ensuring a maximum level of DNI [59].
209 Building Roofs are logical places for efficiently harvesting solar energy [60,61,62,63], therefore roof
210 designs should be optimized to maximize DNI. However, there is still missing literature pointing towards
211 the analysis of DNI of various roof designs before the installation of TSSCs. This requires taking several
212 building-related decision variables including roof types, orientation, and slopes to investigate several
213 optimal building roof designs. Therefore, to assess the actual potential of TSSCs in buildings, their
214 integration with the building envelopes needs to be accurately addressed. This requires developing a
215 parametric model and optimizing building and TSSC designs. Employing such an approach can help
216 to investigate performances of several optimal designs and allow evaluating the trade-offs between
217 each design objective e.g., maximum energy balance, minimum system size, and cost. Therefore, to
218 enable integral designs of building-integrated TSSCs and evaluate several optimal solutions, decision
219 variables related to buildings and TSSCs should be considered in a single design optimization method.
220 Because previous studies either aimed to optimize building roofs to maximize solar gains
221 [2,3,8,9,10,11,12,13,57] or to optimize TSSC configurations [26,27] for improved performance,

concurrent design optimization of both is still missing. This requires an integrated design optimization approach in subsequent phases of the design process that is optimization of roof design followed by optimization of TSSC design across a number of conflicting performance-related objectives. In building energy research, a load match index (LMI) reflecting a match between yield and demand is one of important energy performance indicators [41]. Inspired by previous studies on parametric modeling methods for building-integrated PV [41,42], we intend to increase an annual average LMI (av.LMI) for TSSCs by varying building and system-related design variables. Further, this research envisions that reduced roof space occupied by TSSC modules can lead to cost effectiveness of system where space value is high in urban sector [14].

To this end, we propose a design optimization method by employing a parametric modeling approach by taking several decision variables of both building and TSSCs. Due to their popularity in both, buildings, and solar energy systems, we use NSGA-II as an optimization technique [43,44,45,46]. The proposed design optimization method is based on our previously developed performance assessment method of roof-integrated TSSCs, where several design alternatives are developed by applying parametric modeling approaches [40]. In our previous study, we assessed the performance of several roof-integrated TSSCs by manipulation of the building- and TSSCs-related design parameters i.e., roof shape, roof slope, building orientation, TSSC type, geometric ratio, and separation distance between mirrors. The method presented in this study performs a two-step optimization, first optimizing the building's roof to maximize DNI (single-objective), and then optimizing TSSCs for a number of performance objectives (multi-objective). In multi-objective optimization, the method evaluates av.LMI, and covered roof area. The two-step optimization helps finding optimal roof shape, slope, and orientation as well as optimal TSSC type, solar cell size, number of TSSC modules, geometric ratio, and separation distance between mirrors of TSSCs for good performance. Thus, the method serves to guide decision-makers in the design and operation of TSSCs as part of building geometry as discussed in the following section.

3 The proposed design optimization method

The proposed method is structured in four successive steps (Fig. 1). The first step is the geometric generation step that requires the parametric model creation for roof and TSSC designs considering several decision variables and constraints.

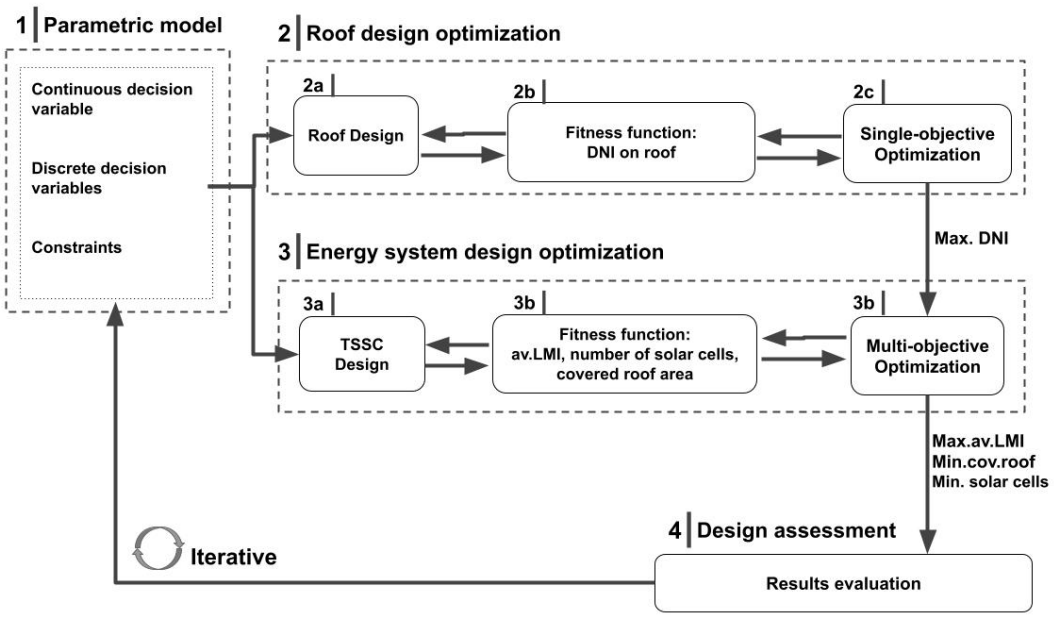

Fig. 1 The proposed design optimization method, where DNI represents the direct normal irradiance, av.LMI represents the annual average load match index, and cov.roof represents the percentage of the available roof area covered by TSSC modules.

The second step is the design optimization of the building roof created in step 1, using a single-objective optimization that aims to maximize the solar irradiance in terms of DNI on the roof. The third step is the design optimization of TSSCs created in step 1 using multi-objective optimization aims to find optimal solutions in terms of two key objectives that are maximizing the av.LMI and minimizing the covered roof area by integrating optimal TSSC designs with optimal roof design created at step 2. The fourth step is the evaluation of generated results to investigate several optimal solutions in terms of av.LMI and covered roof area in the design space. The following sections describe each step in detail.

3.1 Parametric model

In the first step, we assume several design-related (i.e., building dimension) and environmental constraints (i.e., energy demand and weather data), as well as the continuous and discrete type of

272 decision variables based on the variation domains we set (Table 1, Fig. 2, Fig. 3).

273

Table 1 Decision variables, their acceptable range, and types.

Variable(s)	**Lower limit**	**Upper limit**	**Type**
Roof slopes (°)	5	30	Continuous
Building orientation (°)	0	315	Continuous
Geometric concentration ratio	26	122	Continuous
Number of modules	10	100	Continuous
Solar cell width (mm)	7	10	Continuous
Separation distance (m)	0.20	0.71	Continuous
Variable(s)	**Min. index**	**Max. index**	**Type**
Roof type	0	2	Discrete
TSSC type	0	3	Discrete

274

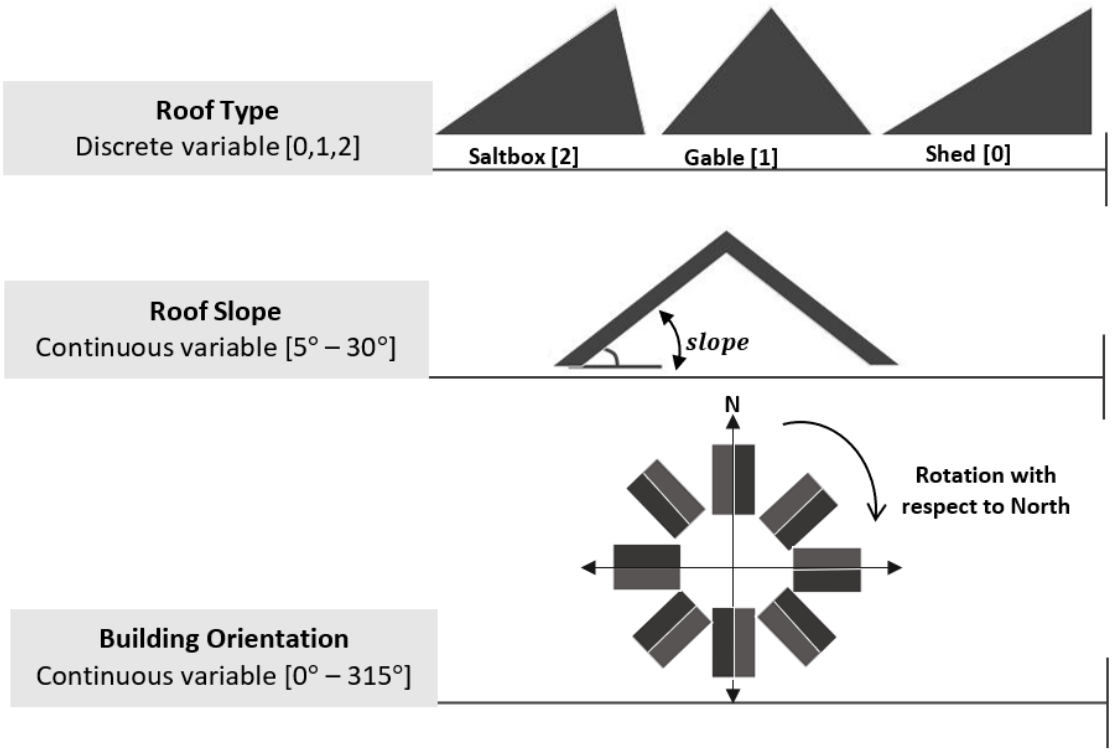

Fig. 2 Continuous and discrete decision variables of roof designs investigated in the method.

275

276

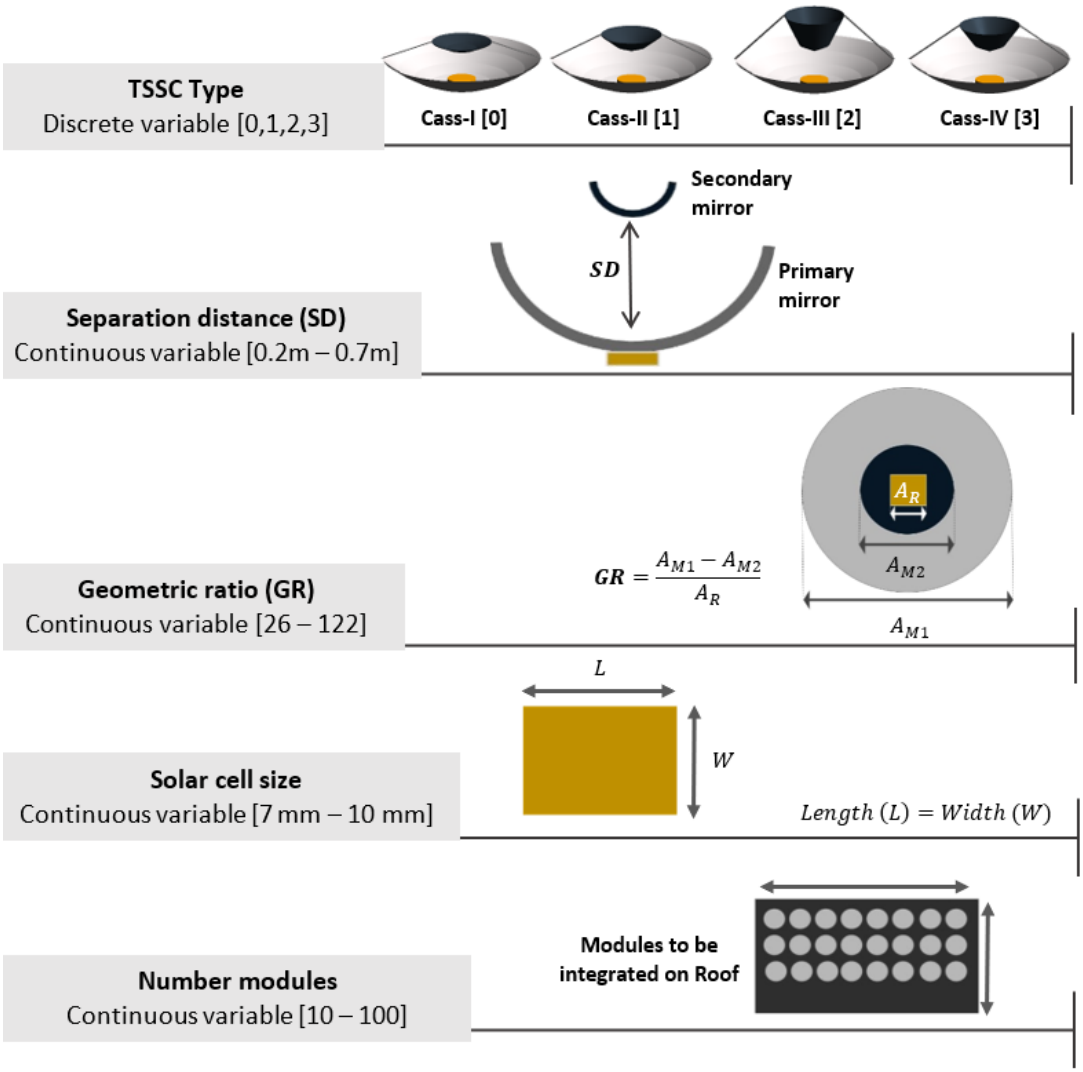

Fig. 3 Continuous and discrete decision variables of TSSC designs investigated in the method, where A_{M1} represents the primary mirror area, A_{M2} represents he secondary mirror area, and A_R represents the receiver area.

In our previous study [40], we considered varying roof type, slope, and orientation, as well as TSSC type, geometric ratio, and separation distance. However, in this study, we further include two design variables related to TSSCs as decision variables that are solar cell size and number of modules [26,27]. The method begins with parametrically generating roof and TSSCs geometries. The roof design is generated based on roof slope and orientation as continuous, and roof type as discrete decision variables (Fig. 2). The scope of this study is limited to three roof types including shed, gable, and saltbox roof. To enable the parametric changes, we assign each roof type with an index as 0 for shed, 1 for gable, and 2 for saltbox roof design. Additionally, TSSC geometries are generated based

on geometric concentration ratio, a number of modules, the width of the solar cell, and the separation distance between mirrors as continuous, and TSSC type as discrete decision variables, with the receiver properties and dimension (i.e., solar cells) as main design constraints (Fug. 3). There are several TSSC design types based on mirror shapes. However, cassegrain design has attracted more attention in solar energy applications as identified by Bushra and Hartmann [22]. In this study, we focus on four cassegrain types as cassegrain employing parabolic primary and secondary mirrors ('cass-I'), cassegrain employing a parabolic primary and a hyperbolic secondary mirror ('cass-II'), cassegrain employing a parabolic primary, and a wide elliptical secondary mirror (cass-III), and cassegrain employing a parabolic primary and a long elliptical secondary mirror (cass-IV). We assign each TSSC type with an index as 0 for 'cass-I', 1 for 'cass-II', 2 for 'cass-III', and 3 for 'cass-IV. After defining parametric relations and creating roof and TSSC designs, the next step is to perform roof design optimization to obtain maximum solar irradiance in terms of DNI as discussed in the following section.

3.2 Roof design optimization

Considering the weather conditions as environmental constraint, this step allows optimizing the roof design by maximizing incoming sunlight on the roof. We use weather data (.WEA) file containing hourly data of the cumulative radiation of a particular geographic location over a certain period. The optimization process through solar simulations uses this data to determine the amount of radiation in particular DNI on a selected roof with respect to roof type, orientation, slope, time range, and shading. We use a genetic algorithm, in particular, NSGA-II for a single-objective optimization that is maximizing the solar energy gain in terms of DNI as given below:

$$Max\ Z_1 = DNI\ (X) \tag{1}$$

Subject to: $X = \{xOrientation,\ xSlope,\ xRoofype\}$

Our method allows estimating hourly, daily, to annually-averaged DNIs, we only focus on annual DNI values because we aim to design a system fulfilling an annual average energy demand. At this step, we define a fitness function for solar assessment analysis on the roof to estimate the DNI. We assign this fitness function to the initial population list with a defined size and apply the optimization algorithm. Then the results transfer to the generation loop to improve the values in each generation.

The generation loop runs the generation and sorting processes until the run iteration counter reaches the limit we set. With different roof design options, we aim to test the maximum solar potential on the roof surface generated at step 1 before integrating TSSCs on the roof.

3.3 Energy system design optimization

Based on the maximum DIN value achieved at the first-step optimization (at step 2), we perform TSSC design optimization at this step. Our primary goal is to design a TSSC as an energy system that can be used for electrical and thermal energy applications in buildings. This step requires information regarding the maximum DNI for optimal roof solutions for step 2. We define fitness functions for two objectives, av.LMI and covered roof area (CRA) as follows:

$$Max\ Z_2 = av.LMI\ (X) \tag{2}$$

$$Min\ Z_3 = CRA\ (X) \tag{3}$$

Subject to: $X = \{xDNI,\ xGeometric\ ratio,\ xSeperation\ distance,$

$xTSSCType, xSolar\ cell\ size, xNumber\ modules\ \}$

The fitness functions measure how good the solution represented by the individual are for the target problem that is to maximize the av.LMI and minimize the covered roof area. The first fitness function is based on electrical and thermal energy calculations. To begin with this, we perform an optical simulation of a TSSC design and estimate the concentration ratio as well as optical efficiency. Then the electrical energy from a TSSC module is estimated (using a solar cell and thermal receiver) as follows [64]:

$$P_{mod,r} = \left((k_t.\eta_c.\tau.[\rho + \frac{1}{CR}.(1 - \frac{\rho}{0.98})].f.\eta_{mod}) - p_{par}\right).\eta_{inv}.CR.DNI.A_{sc}.n_c \tag{4}$$

Where k_t is the power thermal coefficient, η_c is the solar cell efficiency, η_{op} is the optical efficiency, η_{mod} is the module efficiency, η_{inv} is the inverter efficiency, f is the tracking factor, n_c is the number of cells per module, p_{par} is a loss factor (0.023), A_{sc} is the solar cell area, CR is the concentration ratio, τ is the transmittivity of mirrors, ρ is the reflectivity of mirrors, and DNI is the direct normal irradiance. We then calculate the thermal energy yield as [64]:

$$Q_{th,r} = \left(\left[(1-\eta_c.\eta_{mod}.k_t).\eta_{op}.CR.DNI.f\right] - \left[\overline{h_c}.(T_c - T_o) + \epsilon_c.\sigma.(T_c^4 - T_o^4)\right]\right).A_{sc}.n_c \quad (5)$$

where ϵ_c is the cell emissivity and $\overline{h_c}$ is the system working hours, T_c is the cell temperature, T_o is the ambient temperature (25 °C), and σ is the Stefan Boltzmann constant (5.670373*10^{-8} W/m^2.k^4). Finally, this allows estimating overall av.LMI as temporal demand coverage ratio as calculated below [41,42,65]:

$$av.LMI = \frac{1}{N}.\sum_{year} min\,[1, \frac{N_{mod}.g_i(t)}{l_i(t)}] \quad (6)$$

Where N_{mod} is the number of total modules, g is the electrical and thermal yield from a single module, l is the energy load, i is the energy carrier, t is the time interval, and N is the number of data samples. We also estimate the roof covered area (CRA) as the percent of the roof area occupied by modules relative to the total roof area given as:

$$CRA = \left(\frac{A_{mod}.N_{mod}}{A_{roof}}\right).100 \quad (7)$$

Where A_{mod} is the module area, and $\mathrm{A}_{rood=f}$ is the available roof area. We assign the list of fitness functions to the initial population list. Then the results are transferred to a generation loop to improve the values in each generation. The generation loop runs the generation and sorting processes until the iteration counter reaches the defined limit. Thus, the methods allow performing a multi-objective optimization based on decision variables related to TSSC design and the fitness function. In the following step, we assess multiple designs by evaluating multi-objective optimization results.

3.4 Design assessment

This step allows the user to assess several sub-optimal solutions in terms of contradictory objectives by updating the building and TSSC decision variables according to a pre-defined range and moving through the above process described by steps 1 to 3. Thus, in this step, the method reports a set of sub-optimal solutions for the key objectives from two-step optimization. As indicated in previous sections, the key objectives we consider are maximum DNI, maximum av.LMI, and minimum covered roof area. By applying a multi-objective optimization algorithm called a genetic algorithm (NGGA-II) in two subsequent steps, we first seek solutions with the highest DNI, and then we seek a range of

solutions with a trade-off between design objectives that are av.LMI and covered roof area. By doing this, we generate a large design space with several different design solutions. This further automates the process which is essential to be performed on a design from key decision variables as input to the design assessment. The scope of design options is provided by the opportunity to combine different possible values for the decision variables. Hence, our method allows making changes in the optimization settings, and decision variables (i.e., continuous, discrete), and repeating the same process from steps 1 to 3 until we achieve the good or sub-optimal solutions. We validate the method in an illustrative case study as discussed in the following section.

4 Validation approach

To validate the method, we conducted an optimization study for a single-family detached building (size 186 m^2 – 232 m^2) - the most common type of residential buildings in California [66]. As inputs to the model, we considered building- and TSSC-related decision variables (Table 1) as well as several environmental [67] and design constraints (Table 2). We used an hourly cumulative radiation dataset (.WEA file) that is available in Dynamo for the chosen location over a year. We implemented the method using Dynamo [68], SolTrace [69], and R [70] (Fig. 4).

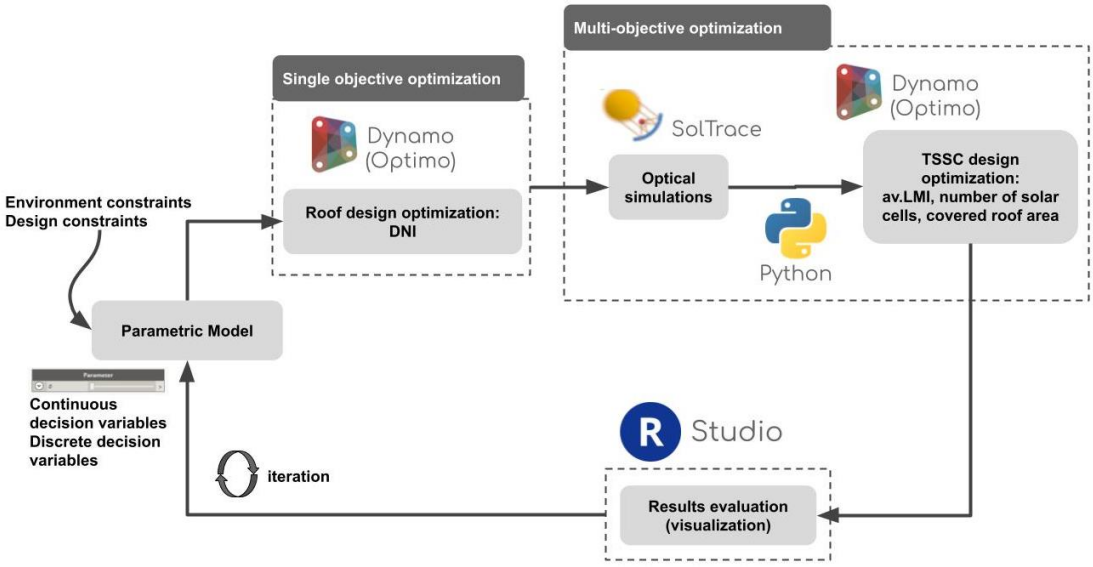

Fig. 4 Implementation of the proposed method.

Table 2 Design and environmental constrains in the method.

Environmental constraints		**Value**	**Design constraints**		**value**
Location:	Latitude	33.61	**Building design:**	Width (W) x Length (L) x Height (H)	16 m x 13 m x 10 m
	Longitude	-114.58		Floor area	208 m^2
Energy demand:	Annual (electrical)	15,545 kWh	**TSSC design:**	module efficiency (η_{mod})	90 %
	Annual (thermal)	7,567 kWh		mirrors transmittivity (τ)	90 %
	Annual total	23,112 kWh		mirrors reflectivity (ρ)	94 %
				Tracking factor (f)	0.9
				cell size (A_c)	81 mm^2
				cell emissivity (ϵ_c)	85 %
				inverter efficiency (η_{inv})	90 %

Dynamo is a visual programming application that allows specifying the design spaces quickly, interactively, and accurately. Calculations were performed in Dynamo using a text-scripting interface. We used the Optimo package in Dynamo was used for single- and multi-objective optimization based on the genetic algorithm (i.e., NSGA-II). SolTrace is an optical ray-tracing tool for optical modeling and simulating of TSSCs, where the Python scripting functionality in Dynamo was used for triggering optical simulations, and for data exchange between SolTrace and Dynamo. R is a programming language for statistical computing and graphics. The implementation begins with the development of a parametric model in Dynamo by generating a random population list of decision variables followed by roof design optimization. At this step, a fitness function is defined for estimating DNI on the roof through Dynamo's solar irradiance analysis package. This analysis is performed over the period of one year (01-01-2020 – 31-12-2020) using the climate data of a chosen location in California. The fitness function for DNI is assigned to the initial population list and finally, the NSGA-II algorithm is applied in Dynamo. This reports the maximum DNI values (single-objective) and corresponding decision variables of the building that are building roof type, roof slope, and orientation. In the following step, TSSC designs are

optimized, where all the calculations are performed in Dynamo. For this, a fitness function is defined that enables the optical simulations of TSSCs in SolTrace. To enable these simulations directly from Dynamo, we developed a python script that triggers optical simulations in SolTrace using the inputs of population generations and optimal DNI. This script also allows exporting all results from SolTrace back to Dynamo. We then calculate the energy yield as well as the required number of modules to meet the energy demand of the building. The fitness function is defined for further estimating the covered roof area by modules that are required to fulfill a specific pre-defined energy demand for a building. The fitness function is assigned to the initial population list and the NSGA-II algorithm is applied in Dynamo. For first- and second-step optimization, the generation loop runs the generation and sorting processes until the iteration counter limit is reached. Finally, the method exports all decision variables and their corresponding results to a comma-separated values (CSV) file. In optimization at steps 2 and 3, the loop could in theory run endlessly unless a defined end criterion is reached. For this study, the end criterion was chosen to be 10 generations with 30 individuals each. We chose the number of generated solutions as a compromise between computational time and having a meaningful number of cases for the optimization algorithm to be able to find sub-optimal solutions. Finally, the results of the optimization study are analyzed graphically in R. Our design problem involves three objectives (i.e., DNI, av.LMI, and covered roof area), thus, we chose to represent our results in Pareto Front. These plots represent the trade-off front between design objectives and allow finding equally optimal solutions as discussed in the following section.

5 Results

Fig. 5 illustrates the results of our design optimization study in parallel coordinate plots that help to explore design space and steer the optimization procedure where each line represents an alternative solution for multiple objectives. Moreover, we also highlight the Pareto optimal solutions (Fig. 6). The first-step optimization of roof design shows that a maximum of annually-averaged DNI of more than 1900 kWh/m^2 is achievable. Thus, maximum DNI is achievable at an optimized roof design that reflects the saltbox roof type (index 2) with a slope of 12^o and orientation of 45.5^o (Fig. 5). This roof design will be considered for the integration of TSSC designs that are optimized using the maximum DNI as an input. During the second-step design optimization, TSSCs are optically simulated under maximum DNI

and for a whole set of the population of input design parameters for different generations. Fig. 6 also shows the design space of all evaluations based on a set of decision variables and corresponding performance objectives well as of Pareto optimal solutions. Moreover, we also represent the trade-off between two objectives, av.LMI versus covered roof area (Fig.6). Our results show that the optimization process can improve the performance of TSSCs and find the sub-optimal solutions from the design space.

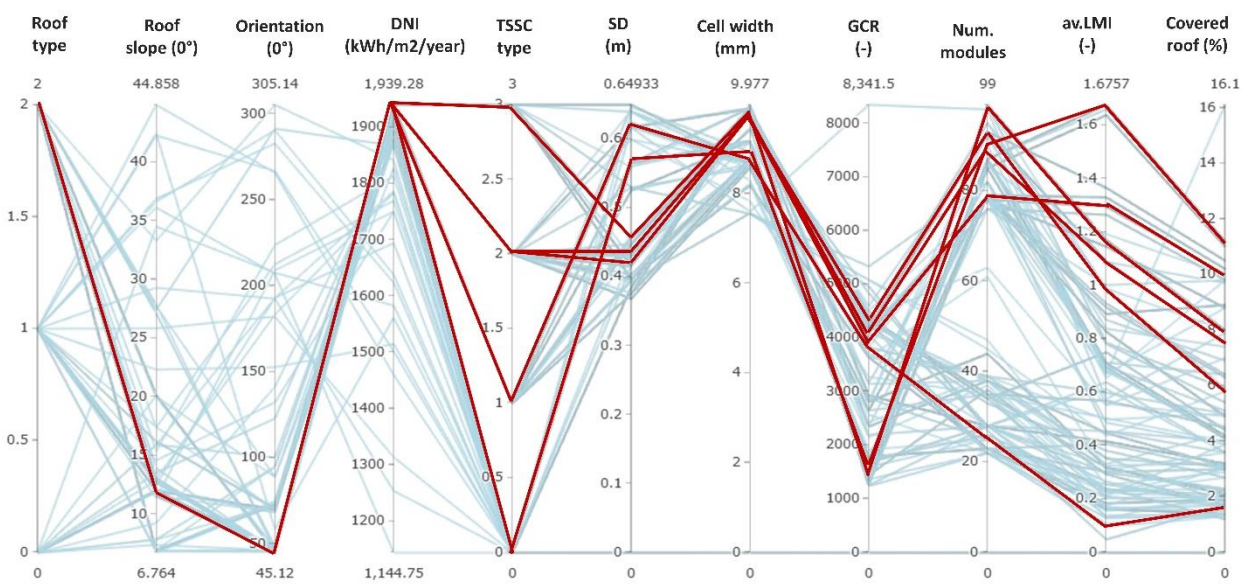

Fig. 5 The design space of all evaluations in three roofs and four TSSC designs, where SD represents the separation distance, GCR represents the geometric concentration ratio, and highlighted design spaces represent sub-optimal solutions for maximum direct normal irradiance (DNI), and annual average load match index (av.LMI), and minimum covered roof area.

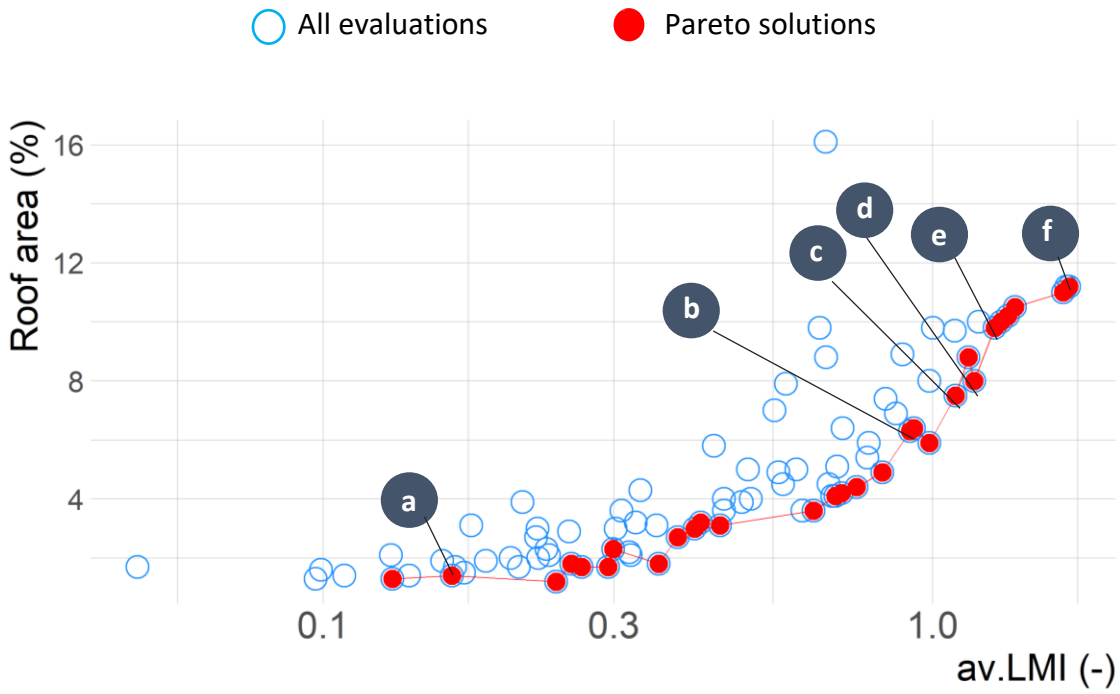

Fig. 6 Pareto optimal solutions for optimization annual average load match index (av.LMI) and covered roof area (%).

Results of the multi-objective optimization (Fig. 6) procedure show that there is a widely distributed initial randomly generated solution set. For the higher generations, the results are getting more and more clustered toward the optimum (Pareto) solution in terms of av.LMI and roof covered area. Moreover, the solution of the final population is better than the solution of the initial population, where Pareto sub-optimal solutions can even provide a high av.LMI of more than 1 and the covered roof area of below 10%. Our results show that very few alternatives of the initial population set satisfy the high-performance criteria to get the maximum av.LMI and minimum roof covered area. However, the higher population set alternatives satisfy these criteria. The Pareto optimal shows a conflicting relationship between performance objectives (Fug. 6), for instance, higher av.LMI leads to a higher number of required modules and ultimately a large fraction of the roof area is occupied by TSSC modules. In Fig. 6 and Fig. 7, we highlight a few good, Pareto sub-optimal solutions representing high-performing TSSC designs that can be integrated with roof design extracted from the first-step optimization process for maximizing the DNI.

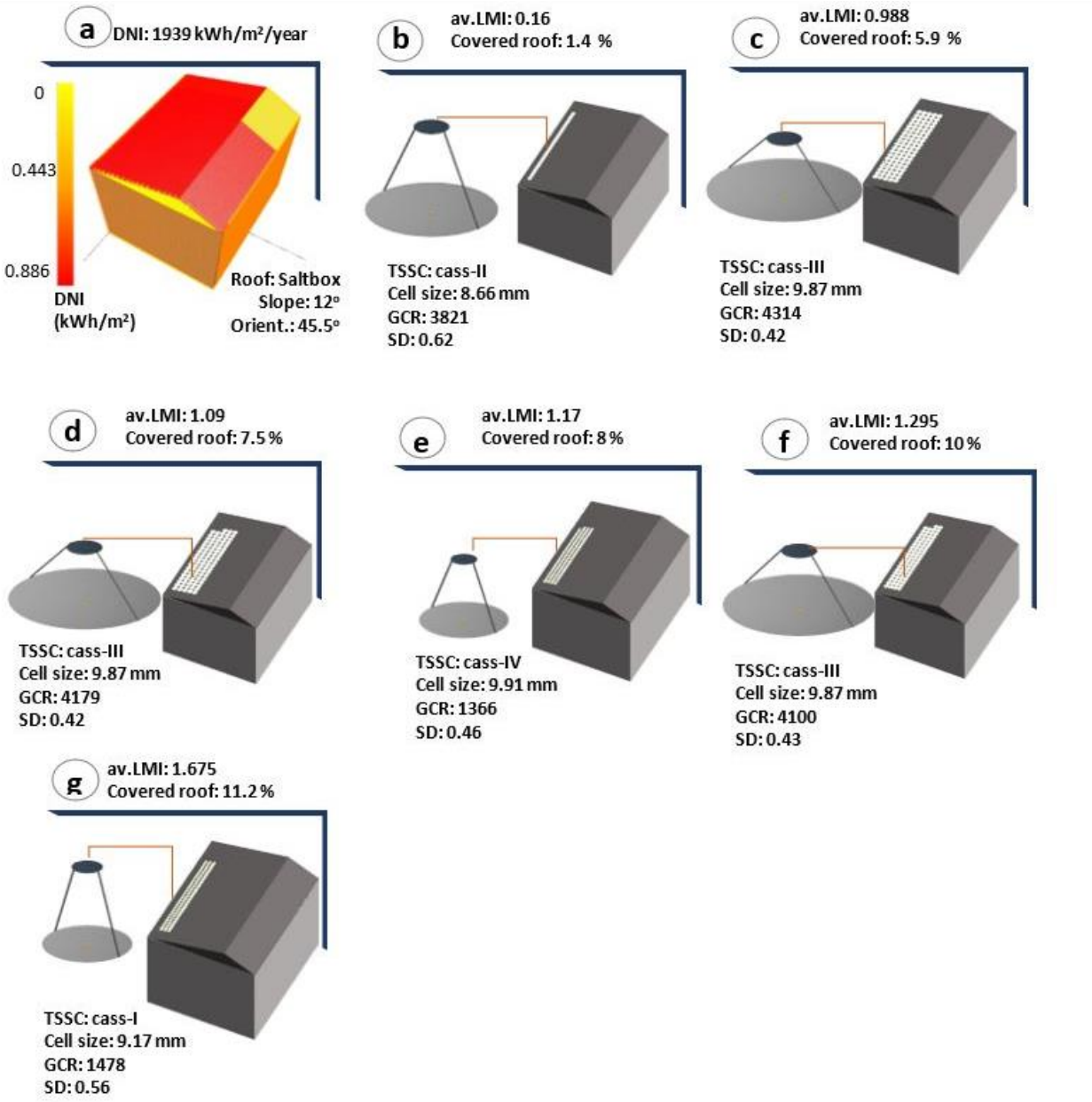

Fig. 7 The design space of all evaluations in three roofs and four TSSC designs for maximum direct normal irradiance (DNI), and annual average load match index (av.LMI), and minimum covered roof area, and number of solar cells (Num.cells), where GCR represents the geometric concentration ratio, and SD represents the separation distance between mirrors.

For instance, the first design alternative (Fig. 7b) consists of TSSC type 1 that is cass-II design (consisting of a parabolic primary and a hyperbolic secondary mirror), with a separation distance of 62 cm, and a geometric concentration ratio of 3821 using 8.66 mm wide solar cell and 23 modules. With this design configuration, the modules cover only 1.4 % of the roof, which is very low, but the av.LMI

503 becomes too small, that is 0.17. Hence, with this design, only 17% of the building energy is met. The
504 second design (Fig. 7c) combined 95 modules of TSSC type 2 that is cass-III design (consisting of a
505 parabolic primary and a wide elliptical secondary mirror), with a wider solar cell receiver (9.9 mm) and
506 the higher geometric ratio of mirrors (4314) compared with the first solution, but with a lower separation
507 distance between mirrors (41 cm). Modules based on this design configuration cover 5.9 % of the roof
508 and lead to av.LMI of 0.98. The third design (Fig. 7d) consists of the same TSSC type, a separation
509 distance between mirrors as and solar cell with the second design but has a slightly lower geometric
510 concentration ratio (4179) and slightly lesser modules (93) and uses slightly small-sized solar cells (9.4
511 mm). This leads to slightly improved av.LMI of 1.1 but covers roof area of 7.5 % due to wider (primary)
512 mirrors. The fourth (Fig. 7e) design consists of TSSC type 3 that is cass-IV design (consisting of a
513 parabolic primary and a long elliptical secondary mirror) using a slightly wider solar cell (9.9 mm), with
514 a slightly larger separation distance (46 cm) and small geometric ratio (1366) compared with previous
515 three designs. Moreover, with a higher number of modules (99) compared with the other three designs,
516 av.LMI can be improved to 1.17 but with a slightly higher covered roof (8 %) compared with other
517 designs.

518 The fifth (Fig. 7f) design is based on the same TSSC type and uses the same width of the solar
519 cell as the second and third design configurations, but with a separation distance of 43 cm and a
520 geometric ratio of 4101. Moreover, with only 78 modules, av.LMI of 1.29 is achievable where roof
521 covered area is 10%. Finally, the last design (Fig. 7g) is of TSSC type 0 that is cass-I (consisting of
522 parabolic primary and secondary mirrors), with a separation distance of 56.4 cm, and a geometric ratio
523 of 1478. With 87 modules, av.LMI of such design is significantly improved to more than 1.5 but covers
524 roof area of more than 10% that is higher among all design configurations. In general, designs shown
525 in Fig. 7d– Fig. 7f show good performance with av.LMI of more than 1 and cover less than 10 % of the
526 roof. However, designs in Fig. 7b and Fig. 7c are good for achieving lower covered roof area but not
527 so good av.LMI values. Further, the design shown in Fig. 7f is impressive in terms of achieving higher
528 av.LMI but the covered roof area increases to more than 10%. In both single- and multi-objective
529 optimization, our results become more clustered and converged at a higher generation size of more
530 than 7. We observed a slight variation in performance objectives at higher generation compared with

initial solutions.

Regarding the simulation time, in our illustrative example, with a generation size of 10, and population size of 30, the simulation time for each generation was 12 minutes, where the overall optimization process took about two hours. The process of parametric model settings, model regeneration, and exporting results took about 10 minutes of the total time. We spent about an hour on first step optimization (roof design for single-objective) and about one hour on second step optimization (TSSC design for multi-objective). This time could be further reduced by running our simulations on a computer with a high computation power. In general, the time consumption and less computation power were the major issues that restricted us to perform optimization for the limited number of generations and population size. Our method offers a unique opportunity for design optimization of building roof and TSSCs, however, the evaluation of our results is limited to the example building. Moreover, there are a few challenges that should be addressed in future studies, as discussed in the following section.

6 Discussion

Our proposed method allows performing a two-step design optimization, where building roof and TSSC geometry can be optimized in consecutive optimization steps. The first-step optimization allows accessing roof design in terms of type, slope, and orientation that can achieve maximum DNI. The second-step optimization allows TSSC design configuration with respect to type, separation distance, geometric ratio, size of the solar cell, and a number of modules, to maximize av.LMI and to minimize roof covered area by modules. The exemplary application shows that the proposed method offers an opportunity for integrative, collaborative, and concurrent design of building geometry and the TSSCs as building-integrated energy systems in the early design stage. Thus, the method aims to help designers to perform a broad variety of simulation-based analyses for design optimization of building and energy system and facilitates performance-driven design generation. The method enables parametric variation in the roof and TSSC design combines multi-objective optimization techniques and suggests calculating several building-related and system-related performance indicators as key objectives. In our previous study, we assessed the performance of several design options by manually manipulating several building-related and TSSC-related design parameters [40]. However, the method

559 proposed in this study demonstrates the process of design space exploration through parametric
560 modeling combined with multi-criteria optimization to find solutions that are good or sub-optimal. The
561 method is demonstrated using a single-family house in California. To understand how the decision
562 variables related to building and TSSCs are driving variables for certain key objectives, we optimized
563 a large design space featuring various combinations of roof slope, orientation, geometric concentration
564 ratio, solar cell receiver's width, number of modules, and separation distance between mirrors in TSSC
565 design as continuous, and roof type and TSSC type as discrete decision variables. Our method helps
566 finding the solutions that are good or sub-optimal in terms of maximizing the DNI as solar gain on
567 building roof, maximizing an av.LMI, and minimizing the covered roof area. The method allows to trade-
568 off between each objective, which can help the decision-making, for example, to decide on which
569 building design gains high solar irradiance, and what are good solutions in terms of high energy yield
570 (i.e., av.LMI), and small covered roof area. The method can serve as a guiding framework for informed
571 decision-making processes where experts from several different domains, such as building architects
572 and energy specialists are involved, having their own, domain-specific concerns. Unlike traditional
573 approaches for modeling such systems, the method proposed in this study allows multi-disciplinary
574 teams to work together towards automatically developing high-performing, self-sufficient building
575 designs, and high-performing energy system designs. The method helps the seamless integration
576 process of integrating TSSCs with building roofs close to satisfying and meeting several key objectives
577 at the same time. By applying multi-objective optimization, the method can significantly support the
578 quick and informed decision-making process by considering several conflicting design-related and
579 performance-related objectives. The method supports incorporating a broader variety of simulations in
580 different domains into the multi-objective optimization methods and leads to a more comprehensive
581 exploration of the solution space and provides better decision support for the designers.

582 However, there exist several key issues that should be addressed in future research. For
583 example, the proposed method is implemented using several tools that include Dynamo for parametric
584 modeling and optimization, SolTrace for optical simulations of TSSCs, Python for bridging SolTrace
585 and Dynamo, and R Cran for graphical representation of results, however, to develop such methods,
586 compatibility among tools remains a key issue. Moreover, the proposed method is not limited to these

587 tools and can be implemented with other relevant tools available to designers and engineers. In this
588 study, we considered energy (i.e., av.LMI), and covered roof area, as key objectives of the system,
589 however, the application of the method can be extended to several other performance-related
590 objectives. For example, the fitness functions in the method can be modified with the inclusion of life-
591 cycle related aspects, environmental, social, or economical aspects. Moreover, we only investigated
592 the building design for higher solar gain in terms of DNI, however, a number of building energy
593 performance objectives could be included which are in conflict with the solar gain in particular surface
594 area to volume ratio (SV). A high SV ratio leads to lower solar gains, and this should also be explored
595 in future research by optimizing the building geometry for example to maximize DNI and minimize the
596 SV value. This could yield valuable insights regarding building energy performance and energy
597 efficiency. Further, the optimization problem can be extended by using several other decision variables
598 related to building design, such as building shape factor, surface area, volume, height, or to system
599 design such as material properties of mirrors and receiver and tracker choices. Further, in the discrete
600 decision variable choices, we considered three roofs (indices of 0 to 2) and four TSSC types (indices
601 of 0 to 3), several other types of building roofs, and design configurations of TSSCs can be added in
602 future research.

603 Moreover, we combined parametric simulations with a specific genetic algorithm-based multi-
604 objective optimization method (NSGA-II). However, several other evolutionary optimization algorithms
605 can also be used in future research which are widely used in building energy research fields such as
606 MOGA [50,51], micro-GA [26,27], MOE [52], GPSOA [53], hybrid-GPSOA [54], and trust-region-
607 reflective least-squares algorithms [55]. Another key issue with our method was that the generation
608 size was limited to 10 and population size to 30, due to limited computation power and large time
609 consumed in each simulation run. This time could be reduced by running the simulations on a high-
610 power computer. Further, the method should be tested for other generation size and/or larger
611 population number and the overall simulation time can be reduced by using cloud computing services.
612 Additionally, we used tools to implement the method which are extensively validated; however, we did
613 not verify the optimization results according to real data. In this study, the workflow is exemplified in
614 the climatic context of California and used the definitions of the USA energy codes for the simulation

parameters. For the purpose of generalization of results, future work should test the proposed method in other climatic contexts and for different decision variables as well as design and environmental constraints. Additionally, the scalability of the proposed method can be extended to multiple buildings and multi-family or multi-story buildings, and to larger districts. This could include the building design optimization with aim of minimizing the shading of roof surfaces as one of design objectives.

7 Conclusions

This research proposes a two-step design optimization method that facilitates the integration process of TSSC geometries with building roofs as renewable energy supply systems. The first-step optimization allows designing an optimal roof for maximum DNI and a second-step optimization allows designing optimal TSSC configurations for maximum energy yield in terms of av.LMI and minimum space requirements in terms of covered roof area by modules. Thus, the method allows the optimal design of both energy autarkic building and energy supply system collaboratively. The method combines optimization algorithms with parametric models of building roofs and TSSC based on a number of decision variables. In the parametric model, we considered several decision variables related to the building (roof type, slope, orientation) and TSSC (type, geometric ratio, solar cell width, module number, and separation distance between mirrors). Moreover, in the parametric model, we applied the optimization algorithm, NSGA-II with an initial population size of 30, and generation of 10, resulting in 330 runs of performance simulation. The proposed method is validated in an illustrative case study of a single-family house (California). The proposed method allows to find a trade-off between conflicting performance objectives in large design space and helps to identify the set of sub-optimal solutions. Our results indicate that the method enables us to assess the performance of different designs and search for the most appropriate design options. Our method helps finding optimal roof and TSSC design configurations in terms of multiple and conflicting objectives. Ultimately, the method can meaningfully support the decision-making process for a low-carbon intensive built environment, where multiple stakeholders can work concurrently and collaboratively.

Acknowledgments

This research did not receive any specific grant from funding agencies in the public, commercial, or not-for-profit sectors.

References

1. Assouline D, Mohajeri N, Scartezzini JL. Quantifying rooftop photovoltaic solar energy potential: A machine learning approach. Sol Energy 2017; 141: 278-296.
2. Youssef AMA, Zhai ZJ, Reffat RM. Genetic algorithm based optimization for photovoltaics integrated building envelope. Energy Build 2016; 127: 627-636.
3. Chen X, Huang J, Yang H. Multi-criterion optimization of integrated photovoltaic facade with inter-building effects in diverse neighborhood densities. Joural of Cleaner Production 2020. DOI: https://doi.org/10.1016/j.jclepro.2019.119269
4. Buonomano A, Calise F, Palombo A, Vicidomini M. BIPVT systems for residential applications: An energy and economic analysis for European climates. Appl Energy 2016; 184(15): 1411-1431.
5. Strzalka A, Alam N, Duminil E, Coors V, Eicker U. Large scale integration of photovoltaics in cities. Appl Energy 2012; 93:413-421.
6. Perera ATD, Attalage RA, Perera KKCK, Dassanayake VPC. A hybrid tool to combine multi-objective optimization and multi-criterion decision making in designing standalone hybrid energy systems. Appl Energy 2013; 107: 412 – 425.
7. Wang C, Kilkis S, Tjernström J, Nyblom J, Martinac I. Multi-objective Optimization and Parametric Analysis of Energy System Designs for the Albano University Campus in Stockholm. Proc Engineering 2017; 180: 621 – 630.
8. Ascione F, Bianco N, Mauro GM, Napolitano DF. Retrofit of villas on Mediterranean coastlines: Pareto optimization with a view to energy-efficiency and cost-effectiveness. Appl Energy 2019; 254: 113705. Doi: https://doi.org/10.1016/j.apenergy.2019.113705
9. Ascione F, Bianco N, Mauro GM, Vanoli GP. A new comprehensive framework for the multi-objective optimization of building energy design: Harlequin. Appl Energy 2019; 241: 331-361. Doi: https://doi.org/10.1016/j.apenergy.2019.03.028

10. Favoino F, Fiorito F, Cannavale A, Ranzi G, Overend M. Optimal control and performance of photovoltachromic switchable glazing for building integration in temperate climates. Appl Energy 2016; 178: 943-961.
11. Taveres-Cachat ET, Lobaccaro G, Goia F, Chaudhary G. A methodology to improve the performance of PV integrated shading devices using multi-objective optimization. Appl Energy 2019; 247: 731-744.
12. Waibel C, Evins R, Carmeliet J. Co-simulation and optimization of building geometry and multi-energy systems: Interdependencies in energy supply, energy demand and solar potentials. Appl Energy 2019; 242: 1661-1682.
13. Liu J, Chen X, Yang H, Li Y. Energy storage and management system design optimization for a photovoltaic integrated low-energy building. Energy 2020; 190. DOI: https://doi.org/10.1016/j.energy.2019.116424
14. Wright DJ, Sana B, Robertson-Gillis C. Micro-Tracked CPV Can Be Cost Competitive with PV in Behind-The-Meter Applications with Demand Charges. Frontiers in Energy Research 2018; 6: 1 – 15. DOI: https://doi.org/10.3389/fenrg.2018.00097.
15. Benda V, Černá L. PV cells and modules – State of the art, limits and trends, Heliyon 2020, 6(12): e05666, ISSN 2405-8440.
16. Shanks K, Baig H, Singh NP, Senthilarasu S, Reddy KS, Mallick TK. Prototype fabrication and experimental investigation of a conjugate refractive reflective homogeniser in a cassegrain concentrator. Sol Energy 2017; 142: 97-108.
17. Price JS, Grede AJ, Wang B, Lipski VM, Fisher B, Lee KT. High-concentration planar microtracking photovoltaic system exceeding 30% efficiency. Nat. Energy 2017; 2:17113. doi: 10.1038/nenergy.2017.113
18. Dai GL, Xia XL, Sun C, Zhang HC. Numerical investigation of the solar concentrating characteristics of 3D CPC and CPC-DC. Sol Energy 2011; 85: 2833-2842.
19. Canavarro D, Chaves J, Collares-Pereira M. A novel Compound Elliptical-type Concentrator for parabolic primaries with tubular receiver. Sol Energy 2016; 134: 383-391.

20. Widyolar B, Jiang L, Abdelhamid M, Winston R. Design and modeling of a spectrum-splitting hybrid CSP-CPV parabolic trough using two-stage high concentration optics and dual junction InGaP/GaAs solar cells. Sol Energy 2018; 165: 75-84.
21. Yew TK, Chong KK, Lim BH. Performance study of crossed compound parabolic concentrator as secondary optics in non-imaging dish concentrator for the application of dense-array concentrator photovoltaic system. Sol Energy 2015; 120: 296–309.
22. Bushra N, Hartmann T. A review of state-of-the-art reflective two-stage solar concentrators: Technology categorization and research trends. Renew Sustain Energy Rev 2019; 114: 1-15. https://doi.org/10.1016/j.rser.2019.109307
23. Canavarro D, Chaves J, Collares-Pereirac M. New second-stage concentrators (XX SMS) for parabolic primaries; Comparison with conventional parabolic trough concentrators, Sol Energy 2013; 92: 98–105.
24. Ullah I, Shin S. Highly concentrated optical fiber-based daylighting systems for multi-floor office buildings, Energy Build 2014; 72: 246–261.
25. Li G, Xuan Q, Akram MW, Akhlaghi YG, Liu H, Shittu S, Building integrated solar concentrating systems: A review. Appl Energy 2020; 260: 1–27.
26. Burhan M, Chua KJE, Ng KC. Sunlight to hydrogen conversion: Design optimization and energy management of concentrated photovoltaic (CPV-Hydrogen) system using micro genetic algorithm. Energy 216; 99:115-128.
27. Burhan M, Shahzad MW, Ng KC. Development of performance model and optimization strategy for standalone operation of CPV-hydrogen system utilizing multi-junction solar cell. International Journal of Hydrogen Energy 2017; 42(43): 26789-26803.
28. Chong KK, Onubogu NO, Yew TK, Wong CW, Tan WC. Design and construction of active daylighting system using two-stage non-imaging solar concentrator. Appl Energy 2017; 45–60.
29. Fernández EF, Montes-Romero J, Casa JI, Rodrigo P, Almonacid F. Comparative study of methods for the extraction of concentrator photovoltaic module parameters. Sol Energy 2016; 137: 413-423.

30. Feuermann D, Mgordon J, Huleihil M. Solar fiber-optic mini-dish concentrators: first experimental results and field experience. Sol Energy 2002; 72(6): 459–472.
31. Kribus A, Zik O, Karni J. Optical fibers and solar power generation. Sol Energy 2000; 68: 405–416.
32. Obianuju ON, Chong KK. High acceptance angle optical fiber based daylighting system using two-stage reflective non-imaging dish concentrator. Energy Proc 2017; 105: 498–504.
33. Sapia C. Daylighting in buildings: Developments of sunlight addressing by optical fiber. Sol Energy 2013; 89: 113–121.
34. Dyson A, Intelligent Facades for High Performance Green Buildings, United States 2017, doi.org/10.2172/1355903.
35. Asl MR, Zarrinmehr S, Bergin M, Yan W. BPOpt: A framework for BIM-based performance optimization. Energy Build 2015; 180:401-412.
36. Wirz M, Petit J, Haselbacher A, Steinfeld A. Potential improvements in the optical and thermal efficiencies of parabolic trough concentrators. Sol Energy 2014; 107: 398–414.
37. Ascione F, Bianco N, Stasio CD, Mauro GM, Vanoli GP. A new methodology for cost-optimal analysis by means of the multi-objective optimization of building energy performance. Energy Build 2015; 88: 78 – 90.
38. Evins R. A review of computational optimisation methods applied to sustainable building design. Renewable and Sustainable Energy Reviews 2013; 22: 230-245.
39. Thompson JD. 3 - Statistical Alignment Approaches. Statistics for Bioinformatics, Methods for Multiple Sequence Alignment 2016, 43-51.
40. Bushra N, Hartmann T, Ungureanu LC. Performance assessment method for roof-integrated TSSCs. Preprint, http://dx.doi.org/10.14279/depositonce-14987. January 2022.
41. Widén J, Wäckelgård E, Lund PD. Options for improving the load matching capability of distributed photovoltaics: methodology and application to high-latitude data. Sol Energy 2009; 83: 1953-1966.

42. Natanian J, Aleksandrowicz O, Auer T. A parametric approach to optimizing urban form, energy balance and environmental quality: The case of Mediterranean districts. Appl Energy 2019; 254: 2-17.
43. Bingham RD, Agelin-Chaab M, Rosen MA. Whole building optimization of a residential home with PV and battery storage in The Bahamas. Renewable Energy 2019; 132: 1088-1103.
44. Hamdy M, Hasan A, Siren K. A multi-stage optimization method for cost-optimal and nearly-zero-energy building solutions in line with the EPBD-recast 2010. Energy Build 2013; 56: 189 – 203.
45. Ferreira AC, Nunes ML, Teixeira JCF, Martins LASB, Teixeira SFCF, Nebra SA. Design of a solar dish Stirling cogeneration system: Application of a multi-objective optimization approach. Applied Thermal Engineering 2017; 123: 646-657.
46. Sanaye S, Sarrafi A. Optimization of combined cooling, heating and power generation by a solar system. Renewable Energy 2015; 80: 699-712.
47. Nguyen AT, Reiter S, Rigo P. A review on simulation-based optimization methods applied to building performance analysis. Appl Energy 2014; 113: 1043-1058.
48. Evins R, Pointer P, Vaidyanathan R, Burgess S. A case study exploring regulated energy use in domestic buildings using design-of-experiments and multi-objective optimisation. Building and Environment 2012; 54: 126 – 136.
49. Asadi E, da Silva MG, Antunes CH, Dias L, Glicksman L. Multi-objective optimization for building retrofit: A model using genetic algorithm and artificial neural network and an application. Energy Build 2014; 81: 444-456.
50. Huang P, Lovati M, Zhang X, Bales C, Hallbeck S, Becker A, Bergqvist H, Hedberg J, Maturi L. Transforming a residential building cluster into electricity prosumers in Sweden: Optimal design of a coupled PV-heat pump-thermal storage-electric vehicle system. Appl Energy 2019; 255. DOI: https://doi.org/10.1016/j.apenergy.2019.113864
51. Khanmohammadi S, Shahsavar A. Energy analysis and multi-objective optimization of a novel exhaust air heat recovery system consisting of an air-based building integrated

780 photovoltaic/thermal system and a thermal wheel. Energy Conversion and Management
781 2018; 172: 595 – 610.
782 52. Lobaccaro G, Chatzichristos S, Leon VA. Solar Optimization of Housing Development.
783 Energy Proc 2016; 91: 868-875.
784 53. Ferreira AC, Nunes ML, Teixeira JCF, Martins LASB, Teixeira SFCF. Thermodynamic and
785 economic optimization of a solar-powered Stirling engine for micro-cogeneration purposes.
786 Energy 2016; 111: 1-17.
787 54. Chen X, Yang H, Peng J. Energy optimization of high-rise commercial buildings integrated
788 with photovoltaic facades in urban context. Energy 2019; 172: 1 – 17.
789 55. Li W, Paul MC, Sellami N, Sweet T, Montecucco A, Siviter J, Baig H, Gao M, Mallick T,
790 Knox A. Six-parameter electrical model for photovoltaic cell/module with compound
791 parabolic concentrator. Sol Energy 2016; 137: 551-563.
792 56. Cajot S, Schüler N, Peter M, Koch A, Maréchal F. Interactive Optimization With Parallel
793 Coordinates: Exploring Multidimensional Spaces for Decision Support. Front. ICT 2019; 5:
794 1 – 28.
795 57. Wu R. Multiobjective optimisation of energy systems and building envelope retrofit in a
796 residential community. Appl Energy 2017; 190: 634 – 649.
797 58. Arteconi A, Zotto LD, Tascioni R, Cioccolanti L. Modelling system integration of a micro
798 solar Organic Rankine Cycle plant into a residential building. Appl Energy 2019a; 251: 1-
799 14.
800 59. Renzi M, Cioccolanti L, Barazza G, Egidi L, Comodi G. Design and experimental test of
801 refractive secondary optics on the electrical performance of a 3-junction cell used in CPV
802 systems. Appl Energy 2017; 185(1): 233–243.
803 60. Kämpf JH, Montavon M, Bunyesc J, Bolliger R, Robinson D. Optimisation of buildings' solar
804 irradiation availability. Sol Energy 2010; 84 (4): 596-603.
805 61. Lobaccaro G, Carlucci S, Croce S, Paparella R, Finocchiaro L. Boosting solar accessibility
806 and potential of urban districts in the Nordic climate: A case study in Trondheim. Sol Energy
807 2017; 149: 347-369.

62. Saretta E, Bonomo P, Frontini F. A calculation method for the BIPV potential of Swiss façades at LOD2.5 in urban areas: A case from Ticino region. Sol Energy 2020; 195: 150–165.
63. Walker L, Hofer J, Schlueter A. High-resolution, parametric BIPV and electrical systems modeling and design. Appl Energy 2019; 238: 164–179.
64. Renno C, Petito F. Design and modeling of a concentrating photovoltaic thermal (CPV/T) system for a domestic application. Energy Build 2013; 62: 392 – 402.
65. Sartori I, Napolitano A, Voss K. Net zero energy buildings: A consistent definition framework. Energy Build 2012; 48: 220-232.
66. EIA, 2017. Household demographics of U.S. homes by housing unit type–2015, U.S. Energy Information Administration (EIA), released on Feb, 2017. (Accessed 10/05/2021).
67. EIA, 2018. Annual household site end-use consumption in the West, totals and averages–2015, U.S. Energy Information Administration (EIA), released on May, 2018. (Accessed 10/05/2021).
68. Dynamo. Open source graphical programming for design. 2019. Available from: http://dynamobim.org/ (Accessed 10/05/2021).
69. Wendelin T. SolTRACE: A New Optical Modeling Tool for Concentrating Solar Optics. Proceedings of the ISEC 2003: International Solar Energy Conference, Hawaii, U.S.A., 2003; 253-260. https://doi.org/10.1115/ISEC2003-44090. March 2003.
70. R Core Team. R: A language and environment for statistical computing. R Foundation for Statistical Computing, Vienna, Austria. 2017. Available from: <https://www.R-project.org/> (Accessed 10/05/2021).